Characterization of a 50kW Inductively Coupled Plasma Torch for Testing of Ablative Thermal Protection Materials Using Non-Air Gases

By

Han All Cha
Department of Aerospace Engineering and Engineering Mechanics
Cockrell School of Engineering

Undergraduate Engineering Honors Thesis

The University of Texas at Austin
May 2018

Noel T. Clemens, Ph.D.
Department of Aerospace Engineering and Engineering Mechanics
First Reader, Supervisor

Philip L. Varghese, Ph. D.
Department of Aerospace Engineering and Engineering Mechanics
Second Reader

Acknowledgements

I would like to thank my supervisor, Dr. Noel Clemens, for making this thesis possible. His guidance and support throughout the entire experiment helped me formulate my objectives while refining the paper presented. His extensive knowledge in the field of fluid mechanics and experience in research allowed me to learn so much about my research topic. I learned how to plan, design, and execute a research experiment, and he solidified my approach every step of the way. I would also like to thank Dr. Philip Varghese, my second reader, for his support in writing the thesis. He provided much help to refine my writing and guided me to approach my experiment by asking the right questions. His feedback throughout helped immensely in completing the thesis. I want to especially thank Benton Greene for the countless hours he spent at the facility to ensure my tests were conducted correctly and for helping me grow as a researcher. While working with him for the past two years, he taught me the fundamentals of the experiment and how a researcher should approach a problem. He has also set up the facility through his previous work, which was essential for me to execute my experimental plans. I would also like to thank Dr. Jeremy Jagodzinski for providing a productive and safe environment for all personnel to work at the facility. Finally, I would like to express my appreciation to Pamela Dahl and Megan McFadden for giving me the opportunity to write and present my undergraduate honors thesis. Their efforts have made the process smooth for all undergraduate honors students. Thank you everyone for all the support. Your help has been critical for me to complete my honors thesis. Through this thesis, I have developed many skills I would never have imagined and feel that I have grown so much as a researcher.

This project is sponsored by NASA JSC under grant number NNX15AH17A.

Characterization of a 50kW Inductively Coupled Plasma Torch for Testing of Ablative Thermal Protection Materials Using Non-Air Gases

Han All Cha
The University of Texas at Austin, 2018

Supervisor: Noel T. Clemens, Ph.D.

Abstract

Thermal protection systems have been a major area of study since the advent of space flight, but recent efforts towards crewed spaceflight missions have placed a new importance on the development of such systems. The 50 kW Inductively Coupled Plasma (ICP) Torch Facility at The University of Texas at Austin allows for rapid testing of high-temperature aerospace materials essential to the development of thermal protection systems in planetary re-entry applications. This ICP Torch Facility has been previously characterized using air as the test gas. However, planets of interest for future exploration have atmospheric compositions that differ from air, so testing heat shield materials in the presence of other gases is critical. To address this disparity between tested and actual environment, the current work characterizes the torch using various combinations of argon, CO_2, and N_2 by determining its operational range at various power settings, mass flow rates, and mixtures these gases. At each setting, the cold-wall heat flux is also measured to determine the range the torch is able to provide. Measurements indicate that using pure Ar gives the torch the largest operating range with regard to power setting and gas

injection mass flow rate, and mixing argon into other gases drastically increases the stable operating range compared to the pure gas. Pure CO_2 does not form a stable plasma discharge, but a mixture of 50% argon and 50% CO_2 (by mass) provides stable operation up to 40 slpm total gas flow rate with a maximum heat flux of 98 W/cm^2. Smaller percentages of CO_2 allow the cold-wall heat flux to be increased to 110 W/cm^2. Pure N_2 forms a stable plasma discharge, but the operating range is very limited, providing stable operation up to 20 slpm total gas flow rate with a maximum heat flux of 110 W/cm^2.

Table of Contents

Nomenclature

$\dot{q}$	=	heat flux
m	=	mass of slug calorimeter
c_p	=	specific heat of slug calorimeter
A	=	exposed surface area of slug calorimeter
$\dot{T}$	=	time rate of change of temperature of slug calorimeter

Chapter 1

Introduction

1.1 Motivation

Planetary re-entry has been a challenge to scientists and researchers for many years. As a spacecraft begins its descent to a planet's atmosphere, it travels at extremely high velocities. For example, typical Mars re-entry velocities are about 14 km/s. During this time, the spacecraft's path lies in the hypersonic regime, which is characterized by the presence of strong aerothermal heating. This heating results in extremely high temperature gases in the shock layer and boundary layers that can reach up to several thousand Kelvin, which causes the atmospheric gas molecules to dissociate and ionize creating a complex mixture of molecules, atoms, and charged particles referred to as a plasma [1]. In many cases the re-entry vehicle is equipped with an ablative thermal protection system (TPS) that acts as a sacrificial layer to protect the vehicle.

Increased space activity and recent efforts for crewed missions have renewed the importance of the TPS to ensure the spacecraft remains intact and the crew safe. In order for missions to be successful with respect to its scientific objectives, a suitable TPS must be lightweight while successfully dissipating the heat experienced upon atmospheric re-entry. A common TPS utilized on a spacecraft is an ablative heat shield attached to the nose of the re-entering vehicle. Ablative heat shields lose mass, which makes them non-reusable. Therefore, full scale flight testing of these systems is difficult and extremely expensive while prediction of these systems requires high-fidelity models of gas-material interactions that need experimental data for validation [2].

With flight tests being very difficult to conduct, heat shield samples are studied in high-enthalpy simulation facilities that are capable of reproducing the same adverse heating conditions experienced during re-entry, such as high-enthalpy flow, heat flux, and Mach number. Producing high-enthalpy flow is essential for testing and qualification of thermal protection materials. To this end, in 2015 a 50 kW ICP torch facility was established at The University of Texas at Austin through a grant from NASA Johnson Space Center.

The facility, pictured in Fig. 1.1, is capable of reproducing the high-enthalpy flow and heat fluxes experienced during re-entry while providing a clean and stable, continuously-operating source of plasma for testing at various input power settings and gas flow rates. Previous work has been conducted on this facility by Greene et al. [2] to characterize the torch using air as the test gas. Greene et al. provided data useful for setting desired torch test conditions, results using emission spectroscopy to determine temperature profiles across the diameter of the plasma plume, and cold-wall heat flux measurements using a slug calorimeter and Gardon gauge.

Figure 1.1: Photograph of the plasma torch facility. without plasma present.

The current paper is an extension of the work of Greene et al. [2], as it further characterizes the plasma torch facility using Ar, N_2, CO_2, and mixtures of these gases to determine the limits of its operational envelope. The study focuses on these three gases because planets of interest for future exploration missions have atmospheric compositions that differ from air, which was previously characterized. The paper also presents heat flux measurements and the variation across the plasma plume at various gas mixtures.

1.2 Research Objectives

The key motivation of this experiment is to characterize the ICP torch to create a more complete baseline of the torch's capability for future heat ablative material testing. The characterization was performed with the following objectives:

1. Determine the operational limits of the ICP torch using Ar, CO_2, and N_2 under the same operating conditions used in the previous work by Greene et al. Each test case will be conducted to determine the range at which the plasma can be sustained using the three specified gases in pure form.
2. Measure the cold wall stagnation point heat flux of the plasma produced by pure Ar, CO_2, and N_2.
3. Measure the cold wall stagnation point heat flux of the plasma produced by the mixtures of the three gases.
4. Verify the presence of an asymmetry in the plasma sustained with gas mixtures by profiling the heat flux variation across the diameter of the plasma plume.

Chapter 2
Background and Literature Review

2.1 Inductively Coupled Plasma Generation

The fundamental design of the ICP is a confinement tube with gas injected at the inlet and the plasma exiting through the nozzle. An ICP torch, depicted in Fig. 2.1, consists of a gas injection inlet, quartz tube, induction coils, and nozzle. The gas is injected into the bottom of the quartz confinement tube that is surrounded by a copper induction coil. ICP torches are powered by high-voltage radio-frequency (a few MHz) AC currents in the coil, which produce an oscillating axial magnetic field.

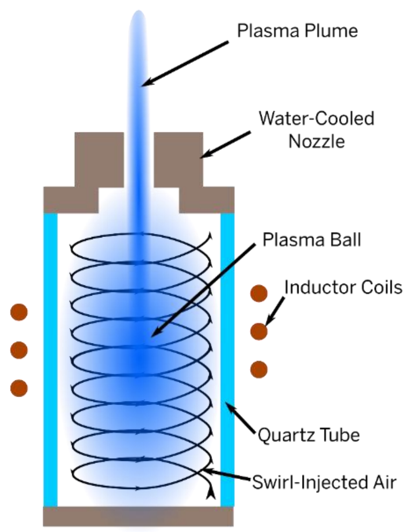

Figure 2.1: Components of the fundamental design of the ICP Torch [2].

After the gas is injected into the plasma chamber, the surrounding oscillating magnetic field with induction lines parallel to the axis of the chamber ionizes the gas atoms and molecules. This is a process known as inductive coupling. During this process, Laux [1] describes that the magnetic field causes the free electrons in the field to radially spin and generate eddy currents, which in turn induces an oscillating electric field. The free electrons in the induction region are accelerated by the force of the electromagnetic field, thus increasing their kinetic energy. These accelerating electrons transfer their kinetic energy to heavy particles in the gas molecules. The plasma becomes self-sustainable once the continuous collision process produces enough electrons in the field. The plasma then issues out of the nozzle producing the plasma plume.

The entire induction heating process occurs in the outer region of the confinement tube, because that is the region where the majority of the electromagnetic energy coupling takes place. The plasma at the central axis of the tube is heated by thermal conduction, convection, and radiation of the heavy gas particles. The particles in the plasma are very high in energy due to energy transfer from the ionizing collisions. Thus, they are driven to lose energy to return to more stable states by two processes: convection and radiation. The particles lose thermal energy through convective heat transfer with the cooled quartz tube. They also lose energy through photon emission, which leads the plasma to be highly luminous. This process produces radiative heating which can be higher than the convective heating rates [1].

2.2 Previous Ground ICP Facilities

Many high enthalpy flow ground facilities designed to replicate the adverse conditions during re-entry have been developed to characterize plasma flows. Facilities capable of making such assessments include arc-jets, pulsed facilities such as shock tubes and shock tunnels, and inductively-coupled plasma torches [3]-[4]. These facilities can duplicate the heat flux experienced in the most difficult re-entry trajectories and the tests enable thermo-chemical process investigations due to their ability to provide steady flow conditions for long durations that exceed that of the re-entry phase. They are capable of producing plasma in steady flow conditions, because steady energy input rates can be maintained for the order of minutes, even hours [5].

Arc-jets are fundamentally heaters with high length-to-diameter ratios segmented into elements. The arc produces a plasma and is magnetically spun to distribute the heat load and reduce electrode erosion. When used for aerospace applications, they rely on a direct arc discharge to produce a high-enthalpy supersonic plasma flow once expanded by a converging-diverging nozzle. Arc-jet produces high heat fluxes, which makes it the preferred method for qualification testing of large-scale TPS materials [5]. For example, Balter-Petterson et al. [6] describes the Aerodynamic Heating Facility (AHF), a 20 MW arc heater, developed in the NASA Ames Research Center. This facility dissociates the injected gas species by an electrical discharge and is accelerated to supersonic flow by expanding it through a supersonic nozzle. The schematic of this facility is pictured in Fig. 2.2. Fletcher et al. [5] also describes the L3K Plasma Tunnel developed by DLR, a 6 MW arc-jet that can produce heat flux rates up to 4 MW/m^2. Both facilities are capable of producing high heat flux rates, but they are contaminated by the electrode material in the stream and are very expensive to operate.

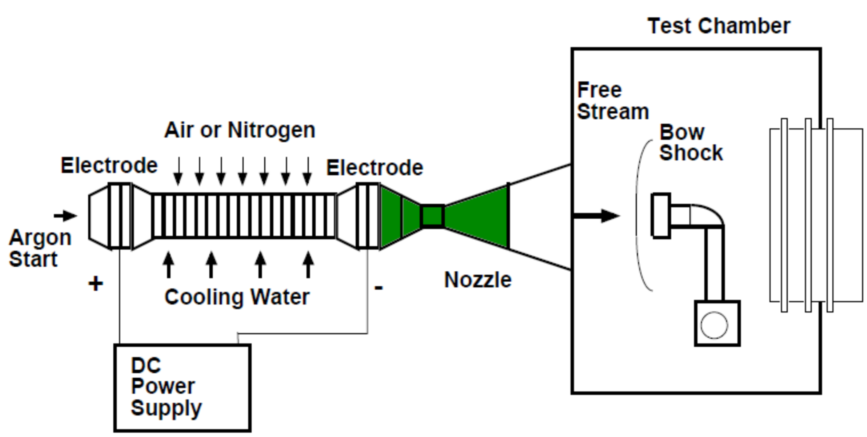

Figure 2.2: Schematic of the AHF arc-jet developed by NASA Ames Research Center [6].

ICP torches can produce both low and high enthalpy flows. Low enthalpy flow torches are designed for material processing, such as fine powder synthesis, spectrochemical elemental analysis, and other large scale industrial applications. High enthalpy flow torches, although operating at low efficiencies, are more suitable for aerospace applications, such as re-entry simulation [5]. In these applications, the stagnation test point conditions from the plasma are dependent on duplicating the total enthalpy, post shock total pressure, and velocity gradient from the hypersonic flight environment.

Knowing the advantages of the ICP facilities, many institutions have developed them to study advanced material reactions with high-temperature flows. Described by Bottin et al. [3], the 1.2 MW plasma wind tunnel or "Plasmatron" was developed at the von Kármán Institute (VKI) in the late 1990's to simulate thermal re-entry conditions for TPS materials used on returning spacecraft. It was part of the Manned Space Transportation Program (MSTP) of the European Space Agency to develop reusable space vehicles. The facility, pictured in Fig. 2.3, is powered using a 1.2 MW, 400 kHz high-frequency generator and the ICP torch had two configurations: one 80 mm diameter torch to test small samples and a 160 mm diameter torch to test large scale TPS tiles. Test articles and sensing probes are mounted on a three-axis support system and the measurements were taken using a Pitot tube and a calorimetric heat flux probe. Samples were tested in a 2.4 m long, 1.4 m diameter test chamber with multiple viewing and insertion ports to allow maximum optical access for plasma characterization [3].

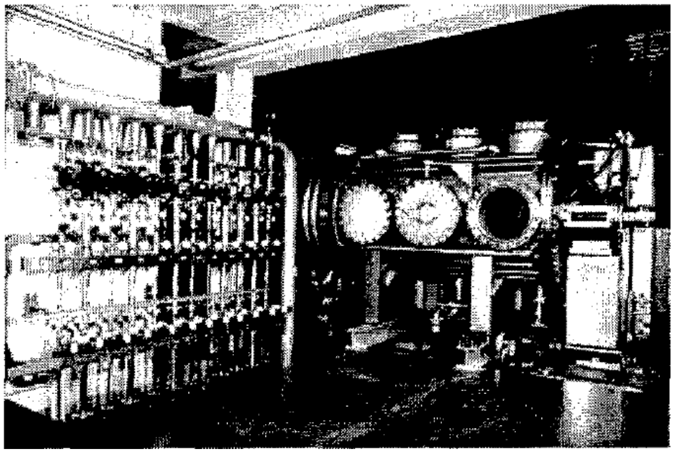

Figure 2.3: The 1.2 MW Plasmatron facility at the von Kármán Institute [3].

In the U.S., Owens [7] describes a 30 kW ICP torch facility that was developed at the University of Vermont to test TPS materials applicable to spacecraft re-entry. Although smaller in scale than the VKI Plasmatron, this facility offers more flexibility and mobility while utilizing a simpler design. Pictured in Fig. 2.4, its components include the RF power supply, induction coil assembly, plasma test chamber, gas feed, and cooling and exhaust systems. The torch is powered up to 30 kW at a frequency between 2.5 to 5 MHz. It is enclosed by a vacuum chamber with multiple optical access with instrumentation and sample ports. This facility offers two configurations to mount and test the sample: the gooseneck design and the brass holder design. Both configurations allow the sample to be inserted into the plasma flow in vacuum but are limited in movement [7].

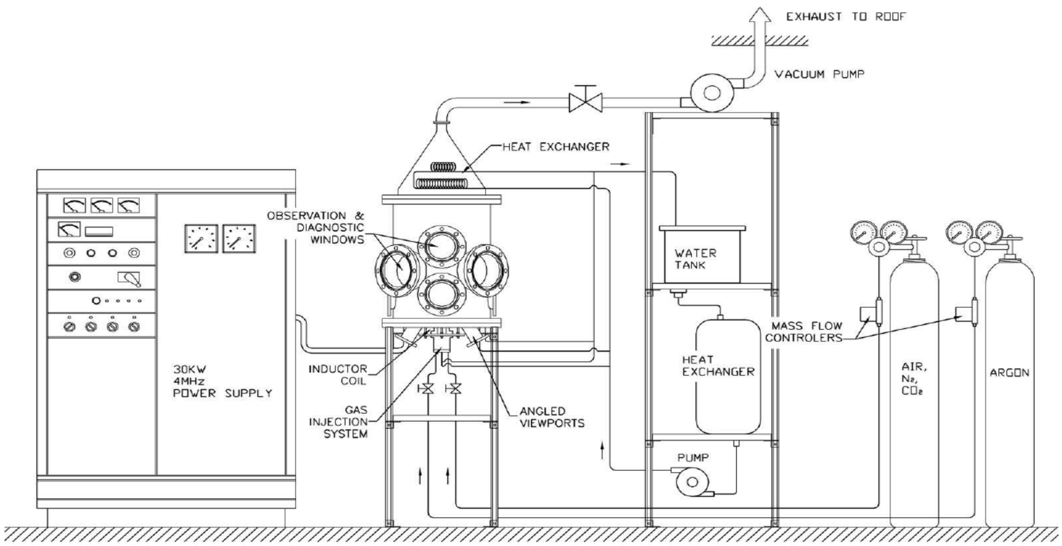

Figure 2.4: Schematic of the 30 kW ICP torch developed at the University of Vermont [5].

Chapter 3

Experimental Facility and Methods

3.1 Experimental Facility

The experiments in this study were performed using the ICP torch facility at the Wind Tunnel Laboratory at the J. J. Pickle Research Campus at the University of Texas at Austin. Because the current work is a continuation of a previous experiment, the facility set up is identical to that of the facility described by Greene et al. [2]. The primary components of the facility are the ICP torch, probe insertion mechanism, and the traverse system depicted in Fig. 3.1. Not shown in the figure are sub-components of the facility such as the pressurized tanks containing the gases, the Plexiglas enclosure for safety measures, the cooling system, power supply, gas injection system, and exhaust ventilation system.

The ICP torch is mounted on a 3-axis traverse system and connected to the power supply by a “flexible tether” [2]. This mobility creates a more effective method of aligning laser-based diagnostic experiments by being able to move the torch into the position of the targeted laser path; however, this was not the objective of this experiment.

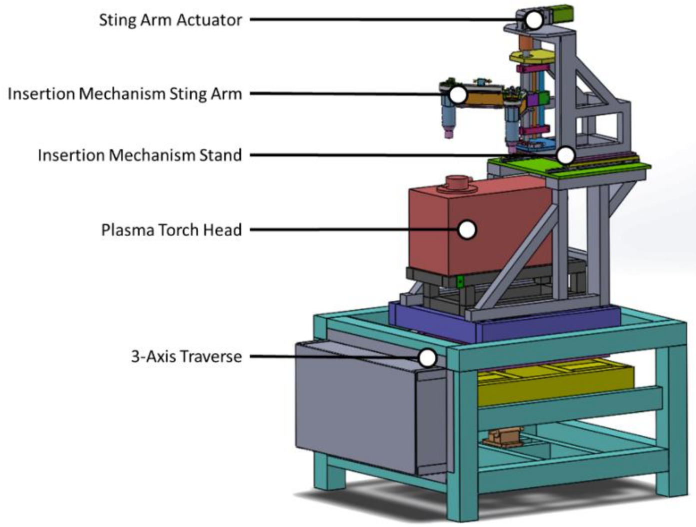

Figure 3.1: A 3-D model of the ICP torch facility outlining its major components [2].

3.1.1 Inductively Coupled Plasma Torch

The ICP torch was developed by Applied Plasma Technologies, which utilizes a 6 MHz, 12 kV AC power supply to couple up to 50 kW of power into the gas stream injected into the torch. The diameter of the torch nozzle is 30 mm, the plasma chamber is 250 mm long and 60 mm in diameter, and the entire system is enclosed by a perforated aluminum housing. The plasma chamber and nozzle are actively water cooled to prevent thermal damage during operation.

The plasma generation and operation are similar to the facility described by Owens et al. [7]. The plasma is generated inside the induction region of the plasma chamber, which is configured by a 3-turn copper induction coil, pressurized spark plug, gas injection system, and a confinement tube. The confinement tube is made up of a quartz outer jacket with a water-cooled copper inner liner. Quartz was chosen because it offers good thermal resistance and its relative transparency to electromagnetic fields. Slots in the copper liner allow penetration of the magnetic field into the chamber. A magnetic field is induced by the helical coil to create the plasma and the coil is internally cooled to prevent arcing from thermal damage during operation, which can lead to plasma coupling inefficiency and damage to the coils. The torch is started by injecting argon into the plasma chamber while the power is supplied at 9.5 kV. Argon is preferred when producing plasma due to its low specific heat, which permits a rapid temperature increase leading to ionization. The spark plug, made up of a graphite rod, is then inserted into the chamber as the initial discharge source and an argon plasma is generated [8]. The gas is then gradually replaced by air, N_2, or another desired test gas. The plasma discharge is sustained by continuous gas injection and RF power supply.

The torch was operated on Ar, N_2, and CO_2 at gas flow rates up to 135 slpm. At higher gas flow rates, the plasma is continuously swept away by the flow in the discharge tube; therefore, it is stabilized with flow recirculation, much like flames are. The torch can utilize two stabilization modes: direct vortex or reverse vortex gas injection. First described by Reed [9], direct vortex stabilization injects a swirling gas at the entrance of the plasma chamber where the flow is injected tangentially. The rotation from this swirl results in a low-pressure area at the center of the chamber, which supports plasma propagation. This in turn causes the plasma to remain at the central axis of the chamber through the centripetal acceleration of the rotating fluid and extends upstream out of the nozzle. The direct vortex injection also allows less heat losses to the cooled wall and helps insulate the chamber walls. The reverse vortex stabilization, described by Gutsol et al. [10], injects the gas at the nozzle end of the chamber, but was not utilized in this experiment due to lower stability when using N_2 and CO_2 as the injection gas.

3.1.2 Probe Insertion Mechanism

The heat flux probes were inserted into the plasma plume through a water-cooled probe insertion mechanism custom built for this facility. The insertion mechanism consists of two arms that rotate smoothly and accurately into the plume, which allows both the slug calorimeter and Gardon gauge to be inserted repeatedly. The mechanism can be programmed to make incremental rotations at constant time steps to automatically scan the heat flux profile across the diameter of the plasma. The two arms are typically utilized to have one probe accurately measure the heat flux of the plume before inserting a test article, but for the purposes of this experiment two different probes were inserted for comparison. The mechanism is driven by a servomotor attached to a sting arm actuator which rotates the two arms by a rate of 45 degrees per second. The mechanism also allows vertical movement of the arms to position the probes and test articles at varying distances from the nozzle exit from 0 mm from the nozzle to 150 mm. In this experiment the vertical position was held constant at 30 mm. The entire mechanism is rigidly mounted onto the torch through a mounting stand, so the location of the probes is constant regardless of the position of the torch. The setup of the probe insertion mechanism is shown in Fig. 3.1.

3.1.3 Traverse System

The plasma torch head is mounted onto a traverse system that allows for three-axes of translation. The system is driven by servomotors and precision ball screw actuators to move the torch to within 0.1 mm accuracy through a range of 150 mm on all three axes. The system can be programmed to make incremental movement at constant time steps to automatically capture the data from multiple locations during a test run. Movement past the edges of the traverse range is prevented by limit switches to prevent collisions with the support structure. Although this system significantly increases the flexibility of the facility for optical diagnostics, it was not essential for the purposes of this experiment.

3.2 Experimental Methods

To meet the objectives of characterizing the torch, the experiment was divided into three methods. First, the operational environment was determined while the plasma was sustained using pure Ar, CO_2, and N_2. Second, the heat flux produced by the plasma using the three pure gases and their mixtures was measured. Lastly, heat flux measurement was profiled across the diameter of the plasma plume to verify the presence of an asymmetry in the plasma plume when the torch was operated under mixtures of the three gases. The three experimental methods are discussed in more detail in the following sections.

3.2.1 Operating Environment

Previous characterization of the torch by Greene et al. [2] resulted in determining the operational envelope of the torch using air as a test gas. The two variables of interest to determine the range were the anode voltage from the power supply and the mass flow rate of the injected air. For this experiment, a similar procedure was followed to determine the operational environment using Ar, N_2, and CO_2 as the test gases.

3.2.2 Heat Flux Measurements

The cold-wall stagnation point heat flux of the plume was measured using two different instruments. The first instrument for measuring heat flux is a Gardon gauge, pictured in Fig. 3.2. The head of the probe was modeled to match the shape of heat-shield samples, and has a diameter of 30 mm. Described by Greene et al. [2], its exterior copper body is water cooled and its center piece consists of a constantan foil disc at the stagnation point of the probe. The thermocouple attached to the probe outputs a millivolt-level signal that is proportional to the heat flux of the plume. The calibration curve provided by Medtherm was used to convert the output signal to heat flux. The water-cooled design of this probe allows for it to be inserted into the plasma for long periods of time and no wait time between each insertion. Owing to this design, the Gardon gauge is often used to measure the heat flux of the plasma before inserting a test article.

Figure 3.2: Image of the Gardon gauge.

The second instrument used to measure the heat flux was the copper slug calorimeter, pictured in Fig. 3.3. Similar to the design of the Gardon gauge, the calorimeter head is 30 mm in diameter to capture the plasma. The copper slug with known properties is attached with a type K thermocouple on its interior surface. This method assumes one-dimensional heat conduction, so the slug is enclosed by a copper housing insulated by a thin air gap between the two components. The calorimeter is not water cooled, so the plasma insertion time is limited to two to four seconds and requires long cool down time between each insertion. The slope of the temperature curve is measured and the time rate of change of the slug temperature, $\dot{T}$, is used to calculate the heat flux of the stagnation region using Eq. 3.1:

$$\dot{q} = \frac{mc_p}{A}\,\dot{T}. \tag{3.1}$$

Here m, c_p, and A is the mass, specific heat, and surface area of the copper slug respectively. As described in the experiment by Greene et al. [2], the mass of the slug is 15.797 g, specific heat is 404 J/kg·K, and A is 2 cm^2. In previous experiments the copper slug was polished following every two insertions due to oxygen reactions, but this was not necessary due to the nature of the gases tested in this experiment.

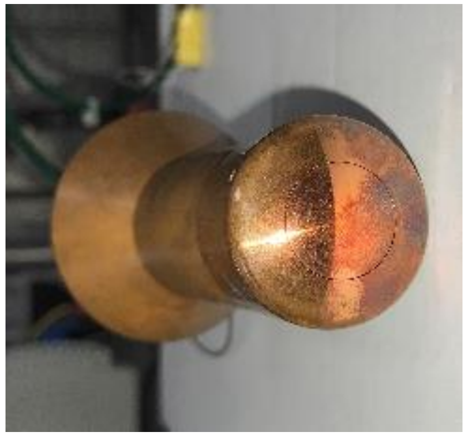

Figure 3.3: Photograph of the surface of the slug calorimeter.

3.2.3 Heat Flux Profile

The heat flux variation across the extent of the plasma plume was profiled using the Gardon gauge, because its cooling system permits long insertion times. The plasma was sustained using a gas mixture of Ar and N_2 and the Gardon gauge was rotated to the edge of the plasma. Using a programmed scan, the Gardon gauge swept across the plasma plume with increments of 5 mm at 3 second intervals. The gauge measured the mean heat flux at each position along the plume. After capturing the heat flux profile, the input parameters were increased, and the heat flux variation was measured again to determine whether the plasma asymmetry changes with increasing gas flow rate and input voltage.

Chapter 4

Analysis and Results

Numerous tests were performed to characterize the torch facility by correlating its outputs as input parameters were varied. In this experiment, different gas compositions were tested while two input parameters were varied: the DC voltage supplied, V, and the mass flow injection rate of the gas into the plasma chamber, $\dot{m}$.

4.1 Operational Environment

The initial tests characterized the capabilities of the torch to determine its operational environment using pure Ar, N_2, and CO_2 as test gases. The two input variables, DC voltage and gas mass flow rate, were varied. For the N_2 and CO_2 cases, the torch was started with Ar injection and once the discharge was established the Ar was slowly replaced by increasing the mass percentage of the desired test gas until reaching 100% or until the torch failed to operate.

The resulting operational environment for Ar is depicted in Table 4.1, which indicates a very large range of operation. The check marks indicate stable torch operation under the two input parameters and the dark regions indicate input ranges at which the discharge could not be sustained. All input parameter ranges between each pair of inputs are assumed to produce stable torch operation. For the Ar case, the electromagnetic field produced below 7.5 kV is not strong enough to sustain the plasma, whereas the upper voltage was limited by the allowable voltage that the torch components can withstand. Mass flow rates below 25 slpm were not tested because the plasma plume height exiting the nozzle was too small to enable a useful measurement, whereas the upper mass flow rate bounds were limited by the plasma becoming too turbulent.

	Mass Flow Rate (slpm)												
Voltage (kV)	**25**	**30**	**35**	**40**	**45**	**50**	**55**	**60**	**65**	**70**	**75**	**80**	**85**
7.5	✓	✓	✓	✓	✓	✓	✓	✓	✓	✓			
8.0	✓	✓	✓	✓	✓	✓	✓	✓	✓	✓			
8.5	✓	✓	✓	✓	✓	✓	✓	✓	✓	✓	✓	✓	✓
9.0	✓	✓	✓	✓	✓	✓	✓	✓	✓	✓	✓	✓	✓
9.5	✓	✓	✓	✓	✓	✓	✓	✓	✓	✓	✓	✓	✓
10.0		✓	✓	✓	✓	✓	✓	✓	✓	✓	✓	✓	✓

Table 4.1: ICP torch operational environment with argon as test gas.

The operational environment for N_2 is depicted in Table 4.2 which indicates a much narrower range of operation. The torch cannot sustain the N_2 plasma below 9.5 kV and the mass flow rates were very limited from 10 slpm to 20 slpm. The torch was able to withstand higher voltages of up to 11.0 kV, but the breakdown process of the gas proved to be more difficult than Ar. At these regions of marginal stability of the torch, the voltage input became very unstable as the efficiency between the coil and plasma dropped significantly.

	Mass Flow Rate (slpm)				
Voltage (kV)	**10**	**15**	**20**	**25**	**30**
9.5	✓				
10.0	✓	✓			
10.5		✓	✓		
11.0		✓	✓		

Table 4.2: ICP torch operational environment with N_2 as test gas.

The operational environment for CO_2 was also investigated. However, the torch was only able to operate until the CO_2 reached a 55% (by mass) mixture with argon. Thus, an operational range for pure CO_2 does not exist for this torch facility.

4.2 Heat Flux Measurements

The cold wall heat flux at the stagnation region of the plasma was measured using the Gardon gauge and slug calorimeter for various experimental conditions. These conditions included the input DC voltage, mass flow rate, and gas mixtures by mass percentage. The measurements were taken at 30 mm downstream of the nozzle exit over the operational envelope. The results of the heat flux measurements using both the Gardon gauge and slug calorimeter at 100% Ar are shown in Fig. 4.1 as a function of mass flow rate. The points indicate individual parameters at which the measurements were taken, and the different marker shapes indicate the distinction between the measurements taken at each respective voltage. It is important to note that the lines connecting the points do not suggest a linear variation between two successive measurements, but rather for ease of view.

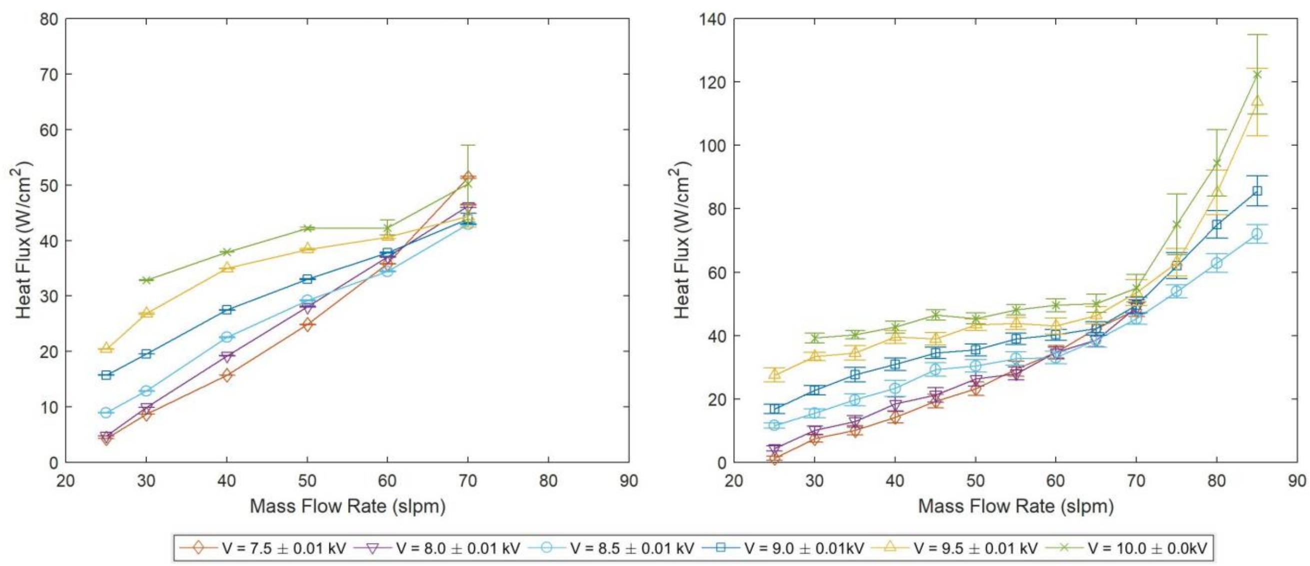

Figure 4.1: Cold wall stagnation point heat flux measurements with increasing mass flow injection rate, parameterized by increasing DC voltage, for 100% argon using the slug calorimeter (left) and the Gardon gauge (right).

Some interesting observations can be made from the results of this test. The heat flux steadily increases with mass flow rate for a given voltage but increases at a higher rate once the mass flow rate goes beyond 70 slpm. This is likely due to the plasma flow becoming more turbulent at higher mass flow rates, which in turn increases the convective heat transfer. The results also confirm that the slug calorimeter and Gardon gauge measure similar heat flux at the same input parameters.

The results of the heat flux measurements using the Gardon gauge at 100% N_2 are shown in Fig. 4.2. The slug calorimeter was not used for this test case due to higher electromagnetic interference associated with using N_2. As with Fig. 4.1, the points indicate measurements at specified inputs and the lines connecting the points are to aid the eye and do not imply a linear trend in the data. Owing to the limited operational envelope when using 100% N_2, few trends can be inferred except that the heat flux increases with increasing mass flow rate and input voltage, as expected. Compared to the argon test, the heat flux measurements produced by the plasma using N_2 were higher at a given voltage even though they were recorded at much lower mass flow rates. For example, the plasma produced using argon with an input of V = 10.0 kV and $\dot{m} =$ 30 slpm resulted in a heat flux of 39 W/cm^2 while the plasma using N_2 with inputs of V = 10.0 kV and $\dot{m} =$ 15 slpm resulted in a heat flux of 65 W/cm^2.

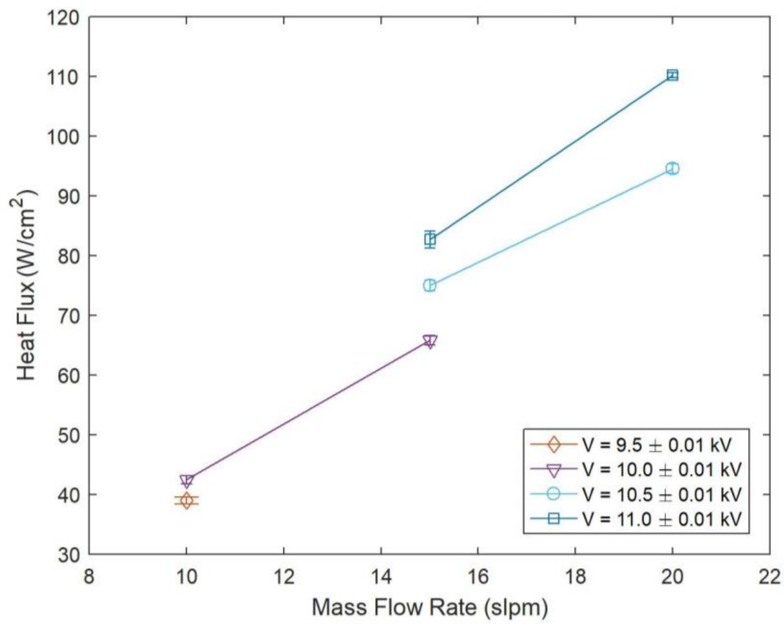

Figure 4.2: Cold wall stagnation point heat flux measurements with increasing mass flow injection rate, parameterized by increasing DC voltage, for 100% N_2 using the Gardon gauge.

The heat flux measurements were also taken using varying mixtures of gases. These mixtures were varied over the range from 0% to 100% at 25% intervals for the argon and N_2 mixture until the N_2 comprised 75% of the mass percentage of the gas injected into the plasma chamber. The results of the heat flux measurements using the Gardon gauge for the Ar/N_2 mixtures are shown in Fig. 4.3, Fig. 4.4, and Fig. 4.5 for the 25%, 50%, and 75% N_2 concentration respectively. The slug calorimeter was not used due to increased electromagnetic interference associated with sustaining the plasma using N_2.

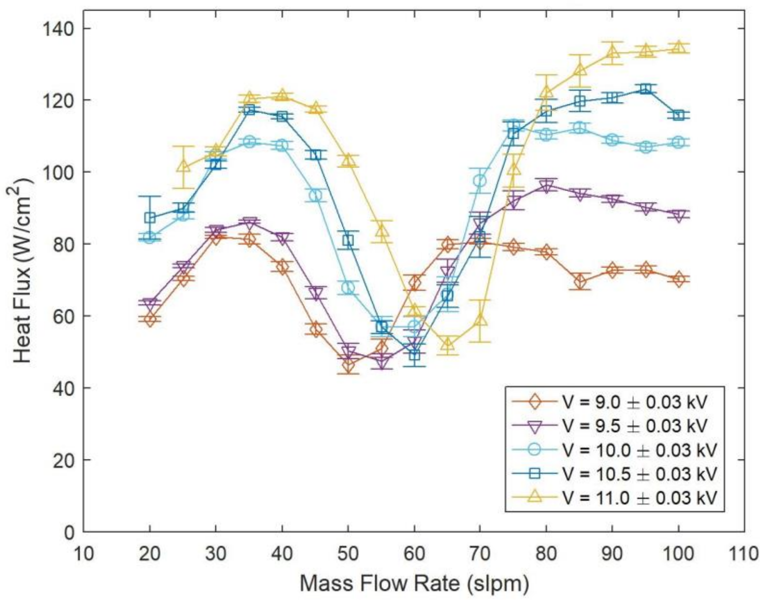

Figure 4.3: Cold wall stagnation point heat flux measurements with increasing mass flow injection rate, parameterized by increasing DC voltage, for 25% N_2 and 75% argon by mass percentage using the Gardon gauge.

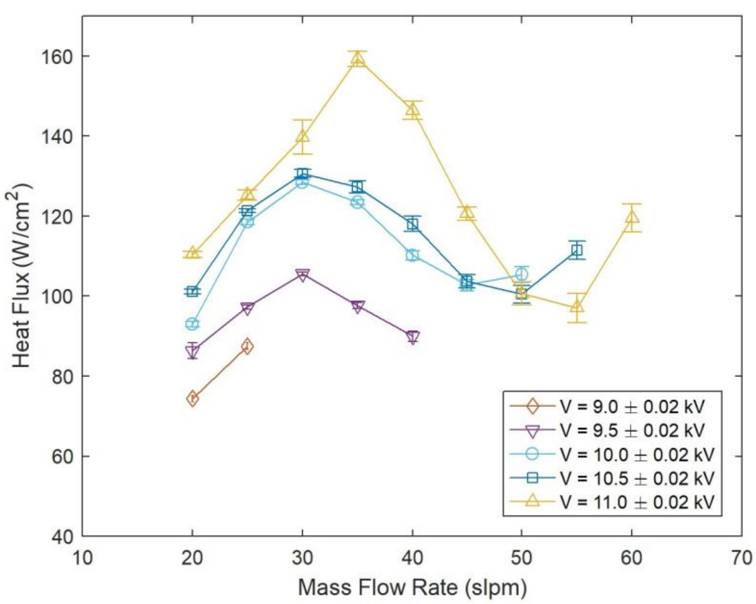

Figure 4.4: Cold wall stagnation point heat flux measurements with increasing mass flow injection rate, parameterized by increasing DC voltage, for 50% N_2 and 50% argon by mass percentage using the Gardon gauge.

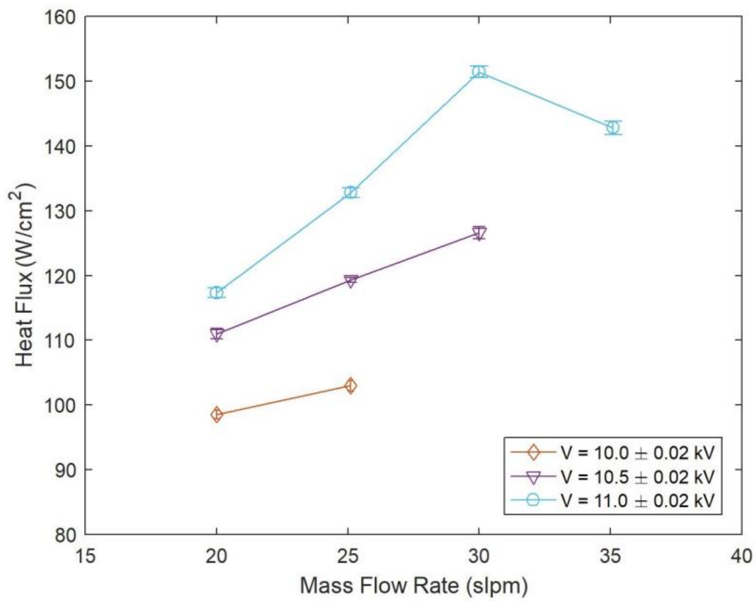

Figure 4.5: Cold wall stagnation point heat flux measurements with increasing mass flow injection rate, parameterized by increasing DC voltage, for 75% N_2 and 25% argon by mass percentage using the Gardon gauge.

The observations from the results correlate to those made in pure gas test cases with respect to the heat flux increasing with increasing input power setting and mass flow rate. The plasma generally produced a higher heat flux at a given power setting and mass flow rate when sustained by a gas mixture than pure gas. The heat flux produced at V = 10.0 kV and $\dot{m} = 70$ slpm at the 25% N_2/75% argon mass mixture was 98 W/cm^2, which is almost twice the amount of the heat flux of 55 W/cm^2 produced with the same input parameters using pure Ar. As more mass percentage of N_2 was mixed into the gas injection stream, the operational envelope also significantly decreased indicating that Ar acts as a stabilizing gas.

The heat flux measurements from the three Ar/N_2 mixtures indicate a general rise in heat flux with increasing N_2 mass percentage. The effect of N_2 concentration on the heat flux is better shown in Fig. 4.6. The heat flux measurements with respect to mass flow rates were plotted at a fixed input power voltage of V = 11.0 kV. Observations indicate that heat flux rises with increasing N_2 mass percentage; however, an inconsistency in the trend appears at $\dot{m} = 40$ slpm. This inconsistency comes from the observed heat flux variation with flow rate across the diameter of the plasma sustained by 25% and 50% N_2 gas mixtures shown in Fig. 4.3 and Fig. 4.4 respectively. There is a significant decrease in the heat flux measured between mass flow rates of 40 and 70 slpm due to an asymmetry within the plasma plume exiting the nozzle of the torch. This creates relatively colder regions away from the plasma center and is referred to as a cold spot.

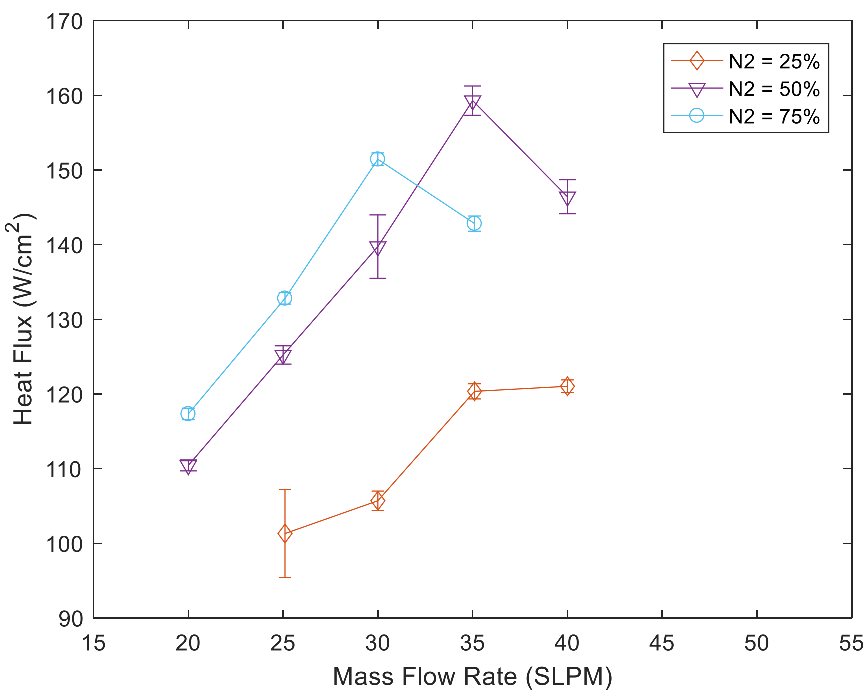

Figure 4.6: Variation of cold wall stagnation point heat flux measurements with mass flow rate, parameterized by increasing N_2 mass percentage. This measurement was taken with input voltage of 11.0 kV.

Heat flux measurements were also taken for varying mixtures of Ar and CO_2. Owing to the mass percentage of CO_2 being limited to 55%, the mixtures were varied over a range from 0% to 50% at 12.5% intervals. N_2 and CO_2 were also mixed resulting in a maximum CO_2 mass percentage of 4%. However, taking heat flux measurements using the N_2/CO_2 gas mixture was not possible due to the mass flow controller's inability to maintain accurate mass flow rates below 5 slpm. The results of the heat flux measurements using the Gardon gauge and slug calorimeter for the Ar/CO_2 mixtures are shown in Fig. 4.7, Fig. 4.8, Fig. 4.9, and Fig. 4.10 for the 12.5%, 25%, 37.5%, and 50% CO_2 concentration respectively.

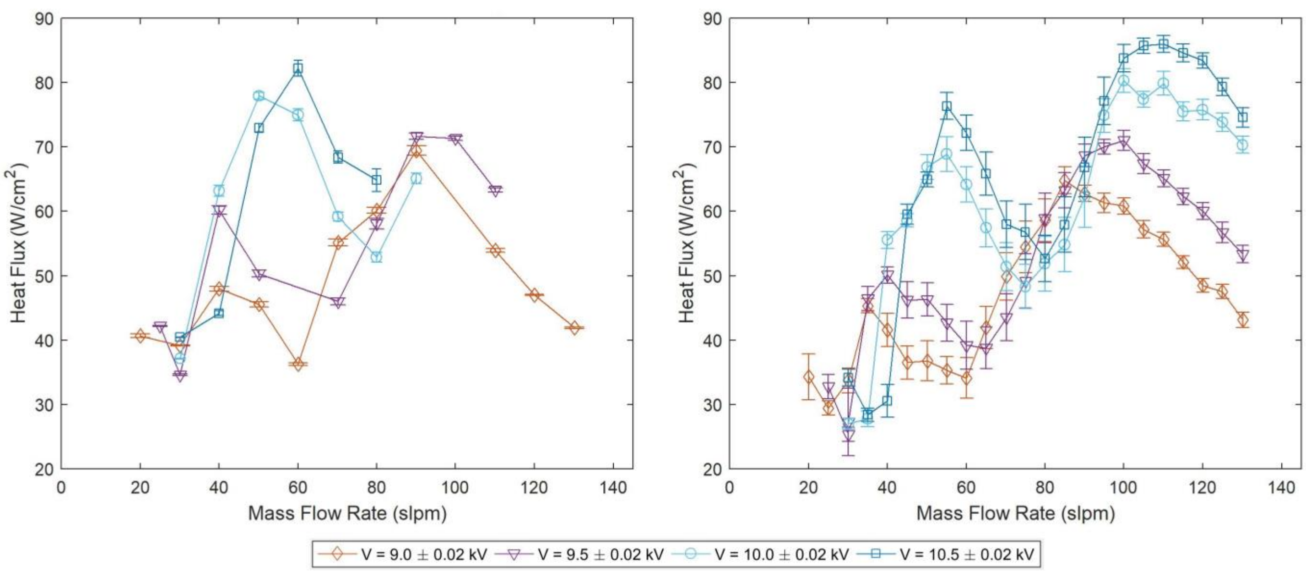

Figure 4.7: Cold wall stagnation point heat flux measurements with increasing mass flow injection rate, parameterized by increasing DC voltage, for 87.5% argon and 12.5% CO_2 using the slug calorimeter (left) and the Gardon gauge (right).

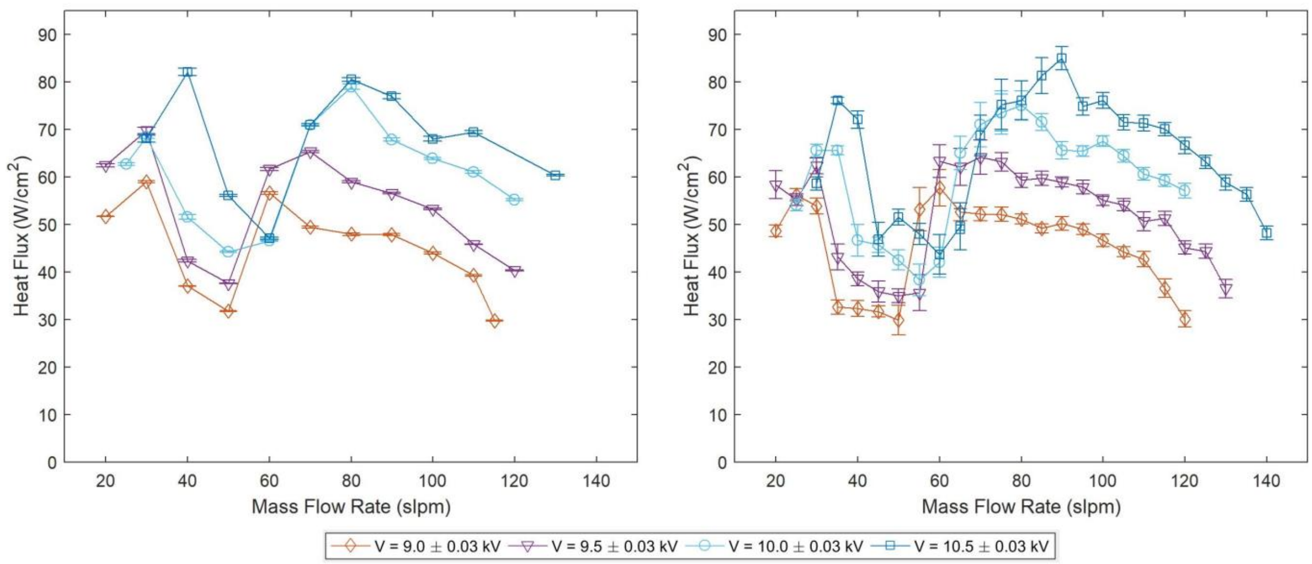

Figure 4.8: Cold wall stagnation point heat flux measurements with increasing mass flow injection rate, parameterized by increasing DC voltage, for 75% argon and 25% CO_2 using the slug calorimeter (left) and the Gardon gauge (right).

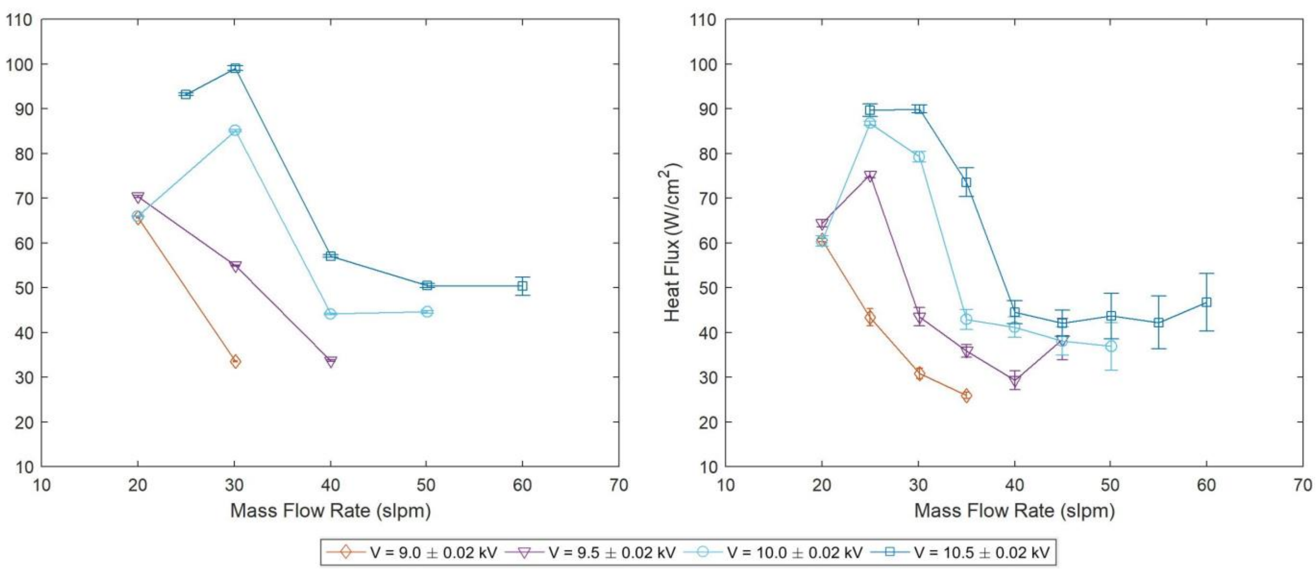

Figure 4.9: Cold wall stagnation point heat flux measurements with increasing mass flow injection rate, parameterized by increasing DC voltage, for 62.5% argon and 37.5% CO_2 using the slug calorimeter (left) and the Gardon gauge (right).

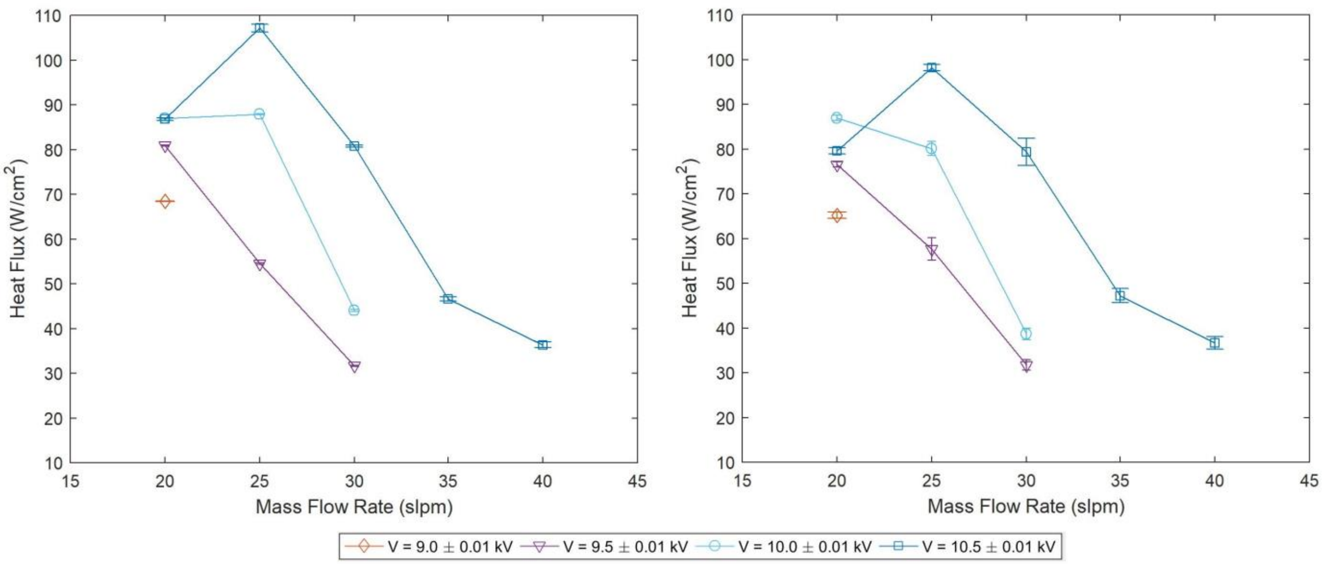

Figure 4.10: Cold wall stagnation point heat flux measurements with increasing mass flow injection rate, parameterized by increasing DC voltage, for 50% argon and 50% CO_2 using the calorimeter (left) and the Gardon gauge (right).

Similar observations can be made from the results using the Ar/CO_2 mixtures. The heat flux for these test cases also increased with increasing voltage and mass flow rate. The plasma produced a higher heat flux at a given voltage setting and mass flow rate when sustained by an Ar/CO_2 gas mixture compared to the pure gas test case. At V = 10.0 kV and $\dot{m} = 70$ slpm for the 25% CO_2/75% Ar mixture, the heat flux was measured at 71 W/cm^2 which is higher than the heat flux produced by the pure Ar gas test case, but lower than the 25% N_2/75% Ar mixture test case. However, the accuracy of the measurements is difficult to determine for certain mass flow rates due to the significant decrease in heat flux as seen similarly in the measurements from the Ar/N_2 gas mixtures.

The significant drop in heat flux drastically decreases the accuracy of the torch's characterization at these specific regions of mass flow rates. This effect is evident in Fig. 4.11 when the heat flux variation with respect to mass flow rates are plotted at a fixed input power voltage of V = 10.5 kV. Fig. 4.7 through Fig. 4.10 indicate a general rise in heat flux with increasing CO_2 mass percentage. However, no such trend exists in Fig. 4.11 when comparing the CO_2 concentrations between $\dot{m} = 20$ slpm and $\dot{m} = 40$ slpm, a region affected by the significant decrease in heat flux. Similar to the Ar/N_2 mixture, the decrease is from nonuniform heat flux variations due to the asymmetry in the plasma, which in turn creates relatively colder regions in the plume. In both gas mixture test cases, the local minimum of the decreasing heat flux region shifts to the right with increasing voltage input suggesting an azimuthal motion of the cold spot about the central axis of the plasma chamber.

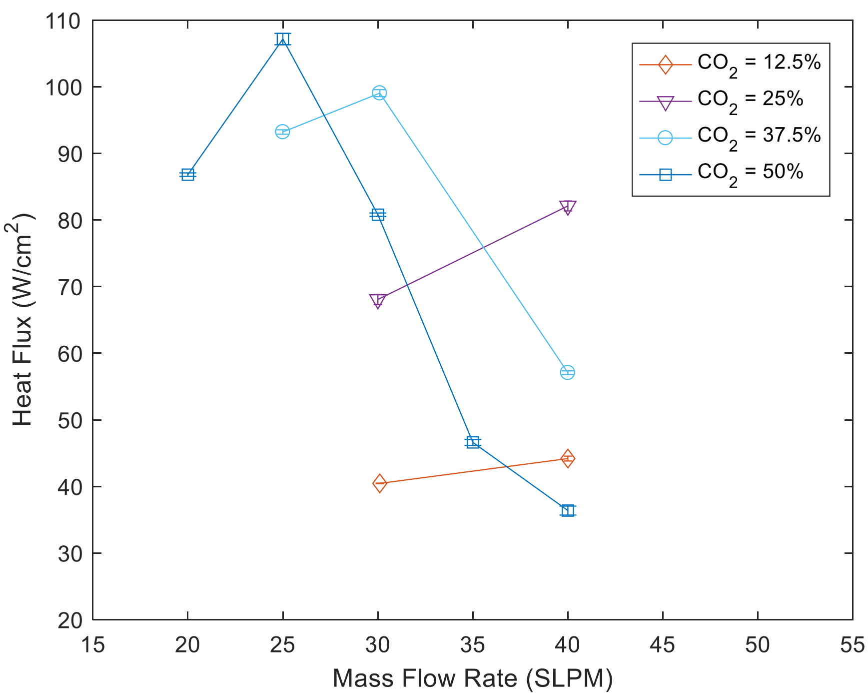

Figure 4.11: Variation of cold wall stagnation point heat flux measurements with mass flow rate, parameterized by increasing CO_2 mass percentage. This measurement was taken with input voltage of 10.5 kV.

4.3 Plasma Asymmetry Profile

The significant decrease in heat flux over certain ranges of mass flow rates was investigated further. The likely explanation of this decrease is the existence of an asymmetric plume when the plasma is sustained by gas mixtures as opposed to pure gases. This asymmetry results in cold spots at certain regions of the plasma. To validate this conjecture the heat flux across a plasma sustained by a 25% N_2/75% Ar mixture was profiled by sweeping the Gardon gage at 5 mm intervals. The heat flux was profiled at two mass flow rates for a given set of two input power settings to show that the cold spot moves azimuthally around the plasma chamber with varying input parameters. These profiles, depicted in Fig. 4.12 and Fig. 4.13, were taken at V = 10.0 kV and V = 11.0 kV and $\dot{m} = 50$ slpm and $\dot{m} = 60$ slpm. The x-axis indicates the position within the plume, with 0 denoting the plume's central axis.

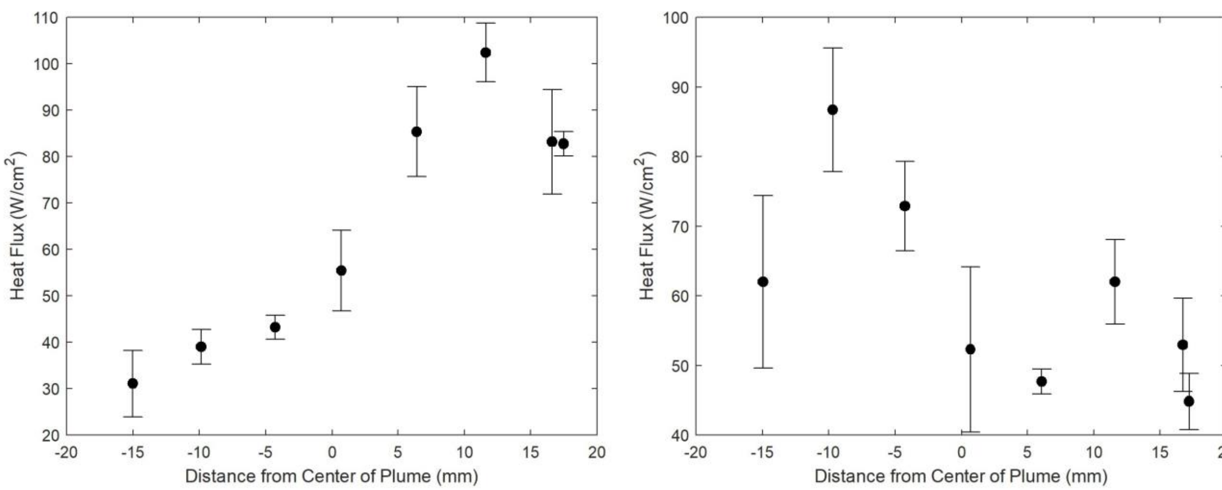

Figure 4.12: Heat flux profile across plasma diameter at V = 10.0 kV with $\dot{\boldsymbol{m}} = \mathbf{50}$ slpm (left) and $\dot{\boldsymbol{m}} = \mathbf{60}$ slpm (right).

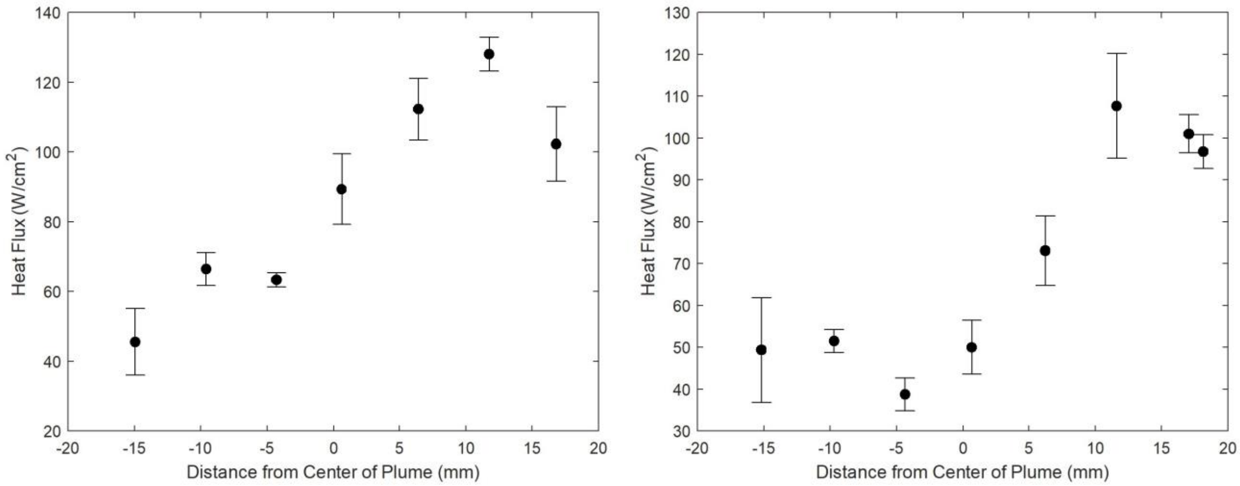

Figure 4.13: Heat flux profile across plasma diameter at V = 11.0 kV with $\dot{\boldsymbol{m}} = \mathbf{50}$ slpm (left) and $\dot{\boldsymbol{m}} = \mathbf{60}$ slpm (right).

The heat flux profiles suggest that the plasma is asymmetric creating a cold region, or cold spot, off-axis from the central axis of the plume. For a plasma with a uniform heat flux variation, the expected profile would show a symmetric variation with the highest heat flux measurement at the center of the plume. The probable cause of the off-axis cold spot in the plasma chamber is the swirl in the gas injection, but the reason for its formation is not known at this time.

Chapter 5

Conclusions and Future Work

5.1 Conclusions

A recently developed inductively coupled plasma torch facility at The University of Texas at Austin was characterized by determining the range of operation conditions and measuring cold-wall stagnation point heat flux using a slug calorimeter and Gardon gage. This experiment was a continuation of a previous work by Green et al. which characterized the torch using air as the test gas. The air was replaced by Ar, N_2 and CO_2 as test gases to reflect atmospheric conditions of other planets targeted by recent and future planetary exploration missions.

The torch successfully operated between an input DC voltage of 7.5 kV and 10 kV and a mass flow rate from 25 slpm to 85 slpm of Ar. It also operated between a voltage of 9.5 kV and 11 kV and a mass flow rate between 10 slpm to 20 slpm of N_2. Operation was successful only up to a 55% CO_2 mass mixture with Ar. The range of operation was much larger for Ar compared to those of N_2 and CO_2.

Heat flux measurements using the slug calorimeter and Gardon gauge resulted in achievable ranges of 5 W/cm^2 to 120 W/cm^2 for pure argon, 40 W/cm^2 to 110 W/cm^2 for pure N_2, 60 W/cm^2 to 155 W/cm^2 for the Ar/N_2 mixture, and 30 W/cm^2 to 85 W/cm^2 for the Ar/CO_2 mixture. When a plasma is sustained using pure Ar or N_2, the heat flux increases with mass flow rate for a given voltage without any signs of leveling off until the torch is no longer operable.

There is a general trend of rising heat flux with increasing N_2 concentration in the gas mixture, but no conclusive trend was determined for the CO_2 concentration.

The results indicated an unexplained decrease in heat flux at regions of moderate mass flow rates when gas mixtures were tested. A profile of the heat flux variation across the diameter of the plasma plume was obtained, which indicated that the decrease in heat flux at these mass flow rates was due to an asymmetry in the plasma creating a relatively cold region. The azimuthal motion of this region about the central axis of the plasma chamber with increasing input parameters is due to the swirl injection of the gas. However, the root cause of the asymmetry is not currently known.

5.2 Future Work and Improvements

The data produced from this experiment serves as a good baseline for further characterization of the torch. The measurements are also helpful in the design of future experiments to test heat shield materials using a plasma sustained by non-air gases. The following will focus on improving the characterization and providing additional work to be conducted in the future.

5.2.1 Eliminate Plasma Asymmetry

A major source of the inaccuracy in the characterization was the presence of an asymmetry in the plasma exiting the nozzle when running under gas mixtures. This led to inconclusive relationships between the heat flux measurements and gas concentrations. Eliminating the asymmetry is essential for not only a more comprehensive understanding of the torch's capability, but also for an accurate baseline when testing thermal protection materials. This asymmetric plasma plume results in a nonuniform heat flux exposure on the test articles which will significantly alter the results. The asymmetry will most likely be eliminated by correcting the nonuniform flow injection at the inlet of the chamber.

5.2.2 Re-characterize Heat Flux Measurements for Gas Mixtures

With the asymmetry in the flow eliminated, the heat flux must be measured again for the gas mixtures to re-characterize the torch at these affected regions. This will provide a more accurate representation of the torch's capability and serve as a better baseline when trying to reach desired heat flux rates at specified gas mixtures. The improved characterization will be important when testing thermal protection materials that will experience specified heat flux rates during re-entry.

5.2.3. Graphite and Teflon Tests

The main purpose of the ICP torch facility is to test thermal protection materials. Previous work has tested graphite and Teflon samples using pure air, Ar, and N_2 plasmas. However, the atmospheric compositions of Earth and many targeted planets for future missions are comprised of these gas mixtures. Testing the materials using pure gases does not fully represent the chemistry occurring on the materials during re-entry trajectories. Further graphite and Teflon tests using the Ar, N_2, and CO_2 mixtures will allow a more complete investigation of the material surface interaction with the plasma. Such tests will include studying material recession and using pyrometry to determine the temperature of the material surface.

References

[1] C. O. Laux, "Optical Diagnostics and Radiative Emission of Air Plasmas," 1993.

[2] B. R. Greene, N. T. Clemens, P. L. Varghese, S. Bouslog, and S. V. Del Papa, "Characterization of a 50kW Inductively Coupled Plasma Torch for Testing of Ablative Thermal Protection Materials," *55th AIAA Aerosp. Sci. Meet.*, no. January, 2017.

[3] B. Bottin, S. Paris, V. V. D. Haegen, and M. Carbonaro, "Experimental and Computational Determination of the VKI Plasmatron Operating Envelope," *30th Plasmadynamic Lasers Conf.*, 1999.

[4] D. G. Fletcher, J. M. Meyers, and W. P. Owens, "University of Vermont Development of a 30 kW Inductively Coupled Plasma Torch Facility for Advanced Aerospace Material Investigations," vol. 298, no. 704, 2012.

[5] D. G. Fletcher and M. Playez, "Characterization of Supersonic and Subsonic Plasma Flows," *25th AIAA Aerodyn. Meas. Technol. Gr. Test. Conf.*, no. June, pp. 1–13, 2006.

[6] A. Balter-Peterson, F. Nichols, B. Mifsud, and W. Love, "Arc Jet Testing in NASA Ames Research Center Thermophysics Facilities," *AIAA Pap. No. 92-5041*, 1992.

[7] W. P. Owens, J. Uhl, M. Dougherty, A. Lutz, J. Meyers, and D. G. Flecther, "Development of a 30 kW Inductively Coupled Plasma Torch Facility for Aerospace Material Testing," *10th AIAA/ASME Jt. Thermophys. Heat Transf. Conf.*, no. 4322, 2010.

[8] A. Cipullo, B. Helber, F. Panerai, L. Zeni, and O. Chazot, "Investigation of Freestream Plasma Flow Produced by Inductively Coupled Plasma Wind Tunnel," *J. Thermophys. Heat Transf.*, vol. 28, no. 3, pp. 381–393, 2014.

[9] T. B. Reed, "Induction-Coupled plasma torch," *J. Appl. Phys.*, vol. 32, no. 5, pp. 821–824, 1961.

[10] A. Gutsol, J. Larjo, and R. Hernberg, "Comparative Calorimetric Study of ICP Generator with Forward-Vortex and Reverse-Vortex Stabilization," *Plasma Chem. Plasma Process*, vol. 22, no. 3, pp. 351–369, 2002.